VALIDATION OF MULTIPLE-SCATTERING CORRECTIONS IN THE ANALYSIS CODE SAMMY

Nancy M. Larson[1]
Oak Ridge National Laboratory
P. O. Box 2008, Oak Ridge, TN 37831-6370 USA
LarsonNM@ornl.gov

Konstantin N. Volev
Institute For Nuclear Research And Nuclear Energy
Bulgarian Academy of Science
Tzarigradsko Shaussee Blvd. N72
1784 Sofia, Bulgaria
bagva@inrne.bas.bg

ABSTRACT

The computer code SAMMY is a tool used in analysis and evaluation of cross section data in the resolved (RRR) and unresolved (URR) resonance region. A brief description of SAMMY's treatment for the URR will be presented, but in this paper we concentrate on the RRR. In the RRR, the code utilizes R-matrix theory (Reich-Moore approximation) to calculate cross sections, corrects those calculated cross sections for a wide variety of experimental conditions (e.g., Doppler and resolution broadening, normalization and background), and employs Bayes' method for fitting experimental data. Of these three operations, correction for experimental conditions is the most cumbersome and least well understood. One particularly difficult but vitally important correction is the multiple-scattering correction for capture and fission yields; exact analytic expressions for those corrections can be formally derived, but cannot be exactly evaluated due to their complexity. Monte-Carlo calculations can provide accurate values for those corrections, but are far too time-consuming for use in analyses such as those performed with SAMMY. Hence it is necessary to use approximate analytic/numerical techniques, and to determine the adequacy of those techniques by comparison with Monte-Carlo simulations. In this paper the approximations employed for multiple-scattering corrections in SAMMY are described and the equations presented. Also described are Monte-Carlo simulations used to validate the accuracy of the SAMMY calculations. Plots are shown comparing the two computations for a variety of experimental situations. Conclusions that can be drawn from these comparisons are (1) the SAMMY implementation of self-shielding and single-scattering corrections are accurate, and (2) the SAMMY implementation of the double-plus scattering correction is generally adequate for thin samples, but there is room for improvement in the more difficult case of thick samples.

"The submitted manuscript has been authored by a contractor of the U.S. Government under contract DE-AC05-00OR22725. Accordingly, the U.S. Government retains a nonexclusive, royalty-free license to publish or reproduce the published form of this contribution, or allow others to do so, for U.S. Government purposes."

[1]1. Corresponding author.

1. INTRODUCTION

Many analyses of neutron-induced cross section data, in both the resolved-resonance region (RRR) and the unresolved-resonance region (URR), have been accomplished using the computer code SAMMY [1,2], developed over the span of two decades at Oak Ridge National Laboratory.

For treatment of the URR, Fröhner's code FITACS [3] was incorporated into SAMMY and modified for increased accuracy and flexibility. This code calculates the cross sections using Hauser-Feshbach theory with width fluctuations; adjustable parameters are s-, p-, and d-wave strength functions, distant-level parameters, average radiation widths (at E = 0), and average fission widths (at E = 0). Energy dependence of the radiation widths is specified via the giant dipole model, of the fission widths via Hill-Wheeler fission barrier transmission coefficients, and of the mean level spacing for *s*-waves via the Gilbert-Cameron composite formula. Mean spacings for $l > 0$ are given via Bethe formula. Moldauer's prescription is used for partial cross sections.

In this paper, we are concerned with only the RRR, in which SAMMY uses the Reich-Moore approximation to R-matrix theory. Accurate analyses in the RRR have significant requirements beyond "merely" using the correct R-matrix formulation with reasonable spin assignments for resonances: It is also necessary to properly include in the calculations all those experimental effects which cause the quantities being measured to differ noticeably from the quantities whose value one wanted to measure. For example, the finite temperature of the sample requires computation of Doppler broadening; spread in beam pulse width and in flight-path-length requires computation of resolution broadening.

(For simplicity, in this paper we confine our comments only to the capture reaction. Readers should keep in mind that these arguments can apply to other reactions as well.)

For analyses of capture measurements, one important experimental effect is the multiple-scattering correction: When a neutron reaches the sample, it is often first scattered by one or more of the nuclei in the sample before it is captured by yet another nucleus. At each scattering, the neutron loses energy. What may therefore be seen in the measurement is not only the resonance peak, but also an additional (smaller) peak at a higher energy; the center of this single-scattering peak corresponds to 90-degree scattering with the exact position determined by kinematics alone. Double- and higher-multiple-scattering peaks also may be visible in the data.

Analytic calculation of the full multiple-scattering correction is not practical, since each additional scattering introduces an additional six-fold embedded integration. The single-scattering correction can be calculated with high accuracy for specific geometries. Double- and higher-multiple-scattering corrections can be calculated with modest accuracy using crude approximations to decouple the integrations. The approximations and computational techniques used in SAMMY are described in the Section 2 of this paper.

Because the computation is complicated, and experimental verification of the results is inconclusive due to the presence of other measurement effects (notably Doppler- or resolution-broadening), it is important

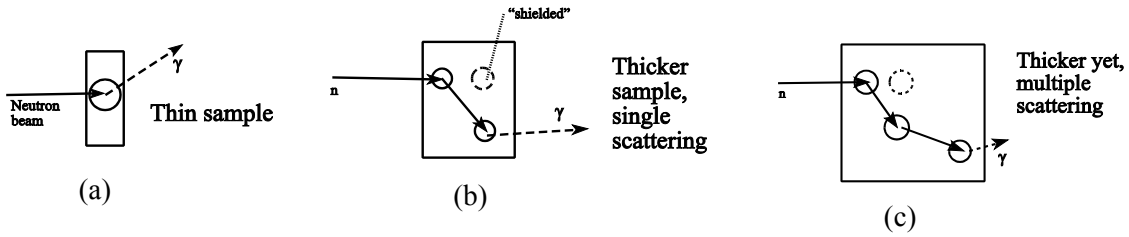

Figure 2. Physical description of capture measurement (a) with no finite-size effects, (b) with self-shielding and single-scattering effects, and (c) with self-shielding and double-scattering effects.

to have an independent method of testing the validity of the SAMMY approximations and computational techniques. Monte-Carlo simulations provide such a method. A Monte-Carlo code SAMSMC has been created, which uses the exact same Doppler-broadened cross sections and geometric information as are used for input to the SAMMY multiple-scattering calculation. Both SAMMY and SAMSMC permit the existence of more-than-one type of nuclide in the sample, and both calculate non-isotropic scattering as needed. Code SAMSMC is described in Section 3.

Both codes provide values of Y_0 (the self-shielded capture yield), Y_1 (the single-scattering correction to the capture yield), and Y_2 (the double- and higher-multiple-scattering correction); the "measured" value is the sum of these three: $Y = Y_0 + Y_1 + Y_2$. (Of course the actual measured value includes resolution broadening and other effects which are neglected in these calculations.) In Section 4 are shown comparisons between results for Y_i ($i = 0, 1, 2$) from SAMMY vs. those from SAMSMC for several types of experiments.

Conclusions and suggestions for future work are presented in Section 5.

2. MULTIPLE SCATTERING CORRECTIONS IN SAMMY

The mathematical formulation of multiple scattering is derived from examination of the geometry of the sample and of the neutron beam; details will be provided in a report to be released later. Three effects (corrections) are considered separately: self-shielding (capture which is not preceded by a scattering), single-scattering (scattering from one nucleus followed by capture in another nucleus), and double-plus scattering (two or more scatterings followed by capture). These effects are shown schematically in Fig.2: The first sketch shows an anomalously thin sample, for which no corrections are needed. In the second sketch, self-shielding and single-scattering are illustrated; double-scattering from a thicker sample is shown in the third sketch.

2.1 SELF-SHIELDING CORRECTION

For the case of very thin samples, each nucleus in the target material has opportunity to "see" neutrons in the incident beam. However, for realistically thick samples, some of the nuclei in the target are effectively hidden in the shadow of other nuclei. Each nucleus experiences an effective neutron flux

equal to the amount transmitted to its position in the sample; integrating over the thickness of the sample gives the observed capture cross section.

This correction is called "self shielding," and always reduces (rather than increases) the observed value of the cross section. The symbol Y_0 is used to represent the self-shielded capture yield:

$$Y_0 = \left(1 - \exp(-n\,\sigma_t)\right) \frac{\sigma_c}{\sigma_t} \tag{1}$$

where n is the sample thickness in atoms/barn, and the subscripts define the type of cross section (capture or total).

Note that there are two common methods for normalizing this quantity: As written in Eq. (1), values for the yield are between 0 and 1. Alternatively, Y_0 may be multiplied by σ_t; in this case, Y_0 approaches the value of the "true" capture cross section in the limit of thin samples. Single- and double-plus scattering yields are normalized in the same fashion.

2.2 SINGLE-SCATTERING CORRECTION

The mathematical description of the single-scattering correction can be written exactly as a six-fold embedded integration over the geometry of the sample and the beam,

$$Y_1(E) = \frac{\int dx \int dy}{S} N \int dz\, \exp(-N\sigma_t z) \int d\Omega\, \frac{d\sigma}{d\Omega}\, \sigma_c' \; N \int dq\, \exp(-N\sigma_t' q) \quad , \tag{2}$$

in which the direction of the beam is assumed to be along the z-axis. The quantity N in Eq. (2) is the atoms/barn thickness n divided by the macroscopic thickness Z in cm (or whatever set of units are chosen). The prime on the capture and total cross sections indicates that these are to be evaluated at the scattered energy E', which is found by kinematics to have the value

$$E' = E\left[\frac{\cos\theta}{(1+r)} + \sqrt{\frac{1}{(1+1/r)^2} - \frac{\sin^2\theta}{(1+r)^2}}\right]^2 \quad , \tag{3}$$

where r is the ratio of the mass of the target nucleus to the mass of the neutron.

If the flat surface of a cylindrical or rectangular sample is perpendicular to the flight path, several of the integrations can be performed analytically. Further simplification requires specific assumptions regarding the shape and size of the sample. For an infinite slab, the equations reduce to an integration over only one variable, μ = the cosine of the angle through which the neutron scattered:

$$Y_4 = 2\pi \int_0 d\mu\, \frac{\sigma'}{\sigma'} \frac{d\sigma}{d\Omega} \left[\frac{1 - e^{-\Sigma_t}}{\sigma} + \frac{e^{-\Sigma_t} - e^{-\Sigma_t'/\mu}}{\sigma - \sigma'/\mu}\right] \quad , \tag{4}$$

and

$$Y_4 \;'\; 2\pi \int_{\&}^{0} d\mu \; \frac{\sigma N}{\sigma N} \; \frac{d\sigma}{d\Omega} \left[\frac{1 \& e^{\& \; F_t}}{\sigma} \;\%\; \frac{e^{\& \; (F_t \& F_t N/:)} \;\& 1}{\sigma \;\& \sigma N/\mu} \right] \;, \tag{5}$$

where the subscripts "*f* " and "*b*" indicate forward and backward scattering, respectively. Y_1 is the sum of both.

The infinite slab approximation, however, is too restrictive for most experiments; samples are generally sufficiently thick that edge effects must be included. Fig. 3 provides a schematic of the path a neutron might take through a cylindrical sample if it is scattered once along the way. In this case, the equations for Y_1 are more complicated:

$$Y_{1c} \;'\; \mathop{m}_{0}^{\mu_1} d\mu \; \frac{d\sigma}{d\Omega} \; \frac{\sigma_c N}{\sigma_t N} \; Q_f(\mu, \sigma_t, \sigma_t N)$$

$$\% \mathop{m}_{\&\mu_1}^{0} d\mu \; \frac{d\sigma}{d\Omega} \; \frac{\sigma_c N}{\sigma_t N} \; Q_b(\&\mu, \sigma_t, \sigma_t N) \tag{6}$$

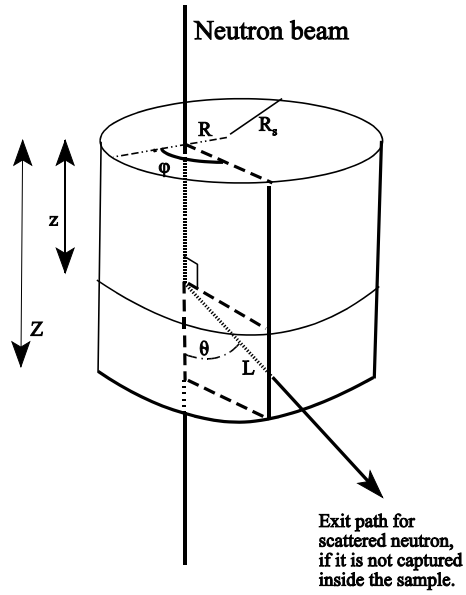

Fig. 3. Geometry for the single-scattering correction to capture or fission yield, for a neutron incident on the flat surface of a cylindrical sample.

where subscript "*c*" on *Y* suggests "corrected by cylindrical edge effects", and where Q_f and Q_b are defined as

$$Q_f(\mu, \sigma_t, \sigma_t N) \;'\; \mathop{m}_{0}^{z_1} dz \; \exp(\& N \sigma_t z) \; U(\mu, z, \sigma_t N)$$

$$Q_b(\mu, \sigma_t, \sigma_t N) \;'\; \mathop{m}_{0}^{z_1} dz \; \exp\big(\& N \sigma_t (Z \& z)\big) \, U(\&\mu, z, \sigma_t N) \tag{7}$$

with *U* given by

$$U(\nu, w, s) \;'\; \& \frac{4N}{R_0^2} \int_{R_1}^{R_0} R \, dR \int_{0}^{\varphi_1} d\varphi \left(\exp\left(\& \frac{Ns(Z \& w)}{\nu} \right) \right.$$

$$\left. \& \exp\left(\& \frac{Ns\left(\& R \cos\varphi \,\%\, \sqrt{R_s^2 \& R^2 \sin^2\varphi} \right)}{\sqrt{1 \& \nu^2}} \right) \right) \tag{8}$$

The limits in these expressions are given by

$$\mu_1 = \cos\theta_1 \qquad \tan\theta_1 = (R_s - R_0)/Z$$

$$z_1 = Z - (R_s - R_0)/\tan\theta$$

$$R_1 = R_s - (Z - z)\tan\theta$$

$$\cos\varphi_1 = \frac{R_s^2 - R^2 - (Z - z)\tan^2\theta}{2\,(Z - z)\,R\tan\theta} \quad . \tag{9}$$

These equations are programmed in SAMMY, with a tabulated array to store Q at specific values of the arguments. Interpolation is then used to calculate Y_{1c} in Eq. (6).

2.3 DOUBLE-SCATTERING CORRECTION

Each scattering prior to capture requires a six-fold embedded integration. Given the complexity of the equations for the single-scattering correction, it is understandable that the equations for two or more scatterings are prohibitively costly to implement and to calculate. It is therefore necessary to use fairly gross approximations in order to evaluate the resulting integrals. The assumptions used within SAMMY are borrowed from Moxon [4], and can be summarized as follows: After a few (two?) scatterings, neutrons are distributed uniformly throughout the sample. Directions of motion for those neutrons are also uniformly distributed throughout the sample. The probability of a neutron escaping from the sample after k scatterings is $e^{-N\sigma^k L}$ where L is the distance from the current location to the edge of the sample. The average escape probability is therefore

$$p_e(E^{(k)}) = \frac{1}{ZN\sigma^{(k)}}\left[\frac{1}{2} - \int_1^4 u^{-3}\,du\; e^{-N\sigma^{(k)}Zu}\right] \tag{10}$$

The full correction for capture preceded by 2, 3, 4, or more scatterings is given (approximately) by

$$\bar{Y}_2(E) = N\int dz\; e^{-N\sigma_t z}\; 2\pi N\int d\mu_1\,\frac{d\sigma}{d\Omega_1}\; y_1\int dq_1\; e^{-N\sigma_t|q_1|} \quad , \tag{11}$$

where the y_i are found iteratively from

$$y_{j-1} = 2\pi\int d\mu_j\,\frac{d\sigma^{(j-1)}}{d\Omega_j}\left(\sigma_c^{(j)} + y_j\right)\left(1 - p_e(E^{(j)})\right) \quad . \tag{12}$$

The superscript j on the cross sections indicates that the cross section is to be evaluated at the energy $E^{(j)}$ after j scatterings.

3. MONTE-CARLO MULTIPLE SCATTERING CORRECTIONS

A Monte-Carlo code for calculation of multiple-scattering corrections for capture measurements was written originally by deSaussure [5] and modified by Perey [6]. For this work the code (now called SAMSMC) has been extended to include a number of features not present in the original: (1) non-isotropic scattering; (2) multiple nuclides in the experimental sample; (3) use of SAMMY-calculated Doppler-broadened cross sections as input to ensure that both codes are calculating the same quantities; (4) output of the three components Y_0, Y_1, and Y_2 separately; (5) output for graphical comparisons of results.

4. COMPARISON OF ANALYTIC AND MONTE-CARLO CALCULATIONS

The first example is for a solitary nuclide, ^{58}Ni, in a relatively thin sample. Figure 4a shows the relative size of the self-shielded capture yield (dotted curve), the single-scattering correction (dashed curve), and the double-plus scattering correction (lower solid curve); the capture yield (sum of the other three) is the top solid curve. In the two smaller figures, the dashed curve represents the SAMMY analytic calculation and the solid curve the SAMSMC Monte-Carlo calculation for (part b) single-scattering and (part c) double-plus-scattering corrections. The dashed curve for single-scattering is almost entirely obscured by the solid curve, indicating that there is little difference between analytic and Monte-Carlo results. For double-plus scattering, there is a small but noticeable difference. This is true in most of the examples studied thus far, and reflects the limitations of the approximations inherent in the uniform-distribution approximation.

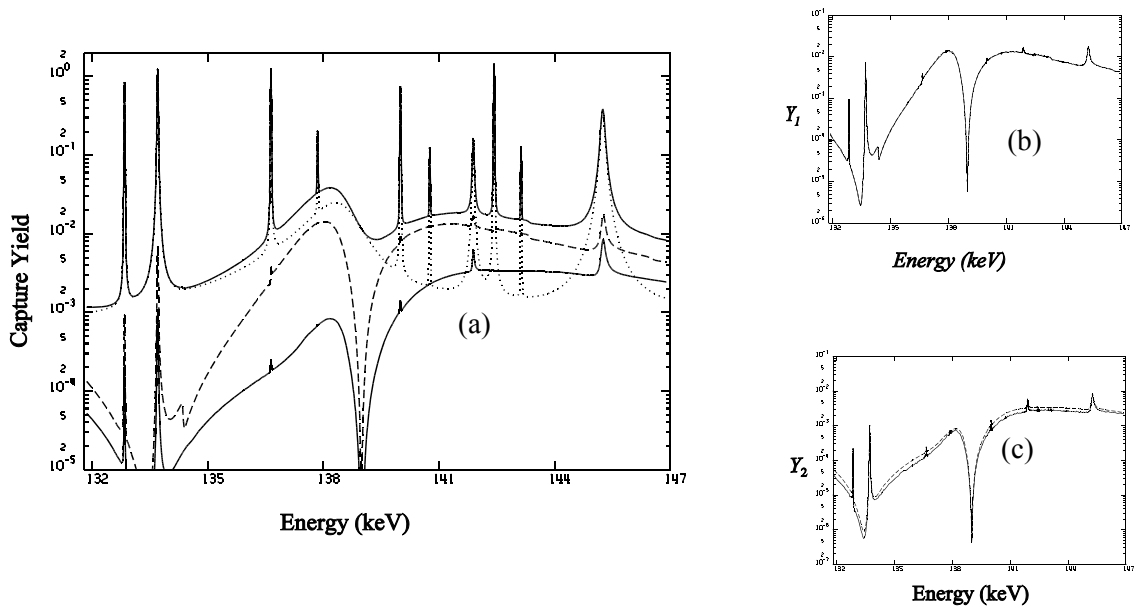

Figure 4. Capture yield for ^{58}Ni with sample thickness 0.03820 atoms per barn. See text for details of the plots.

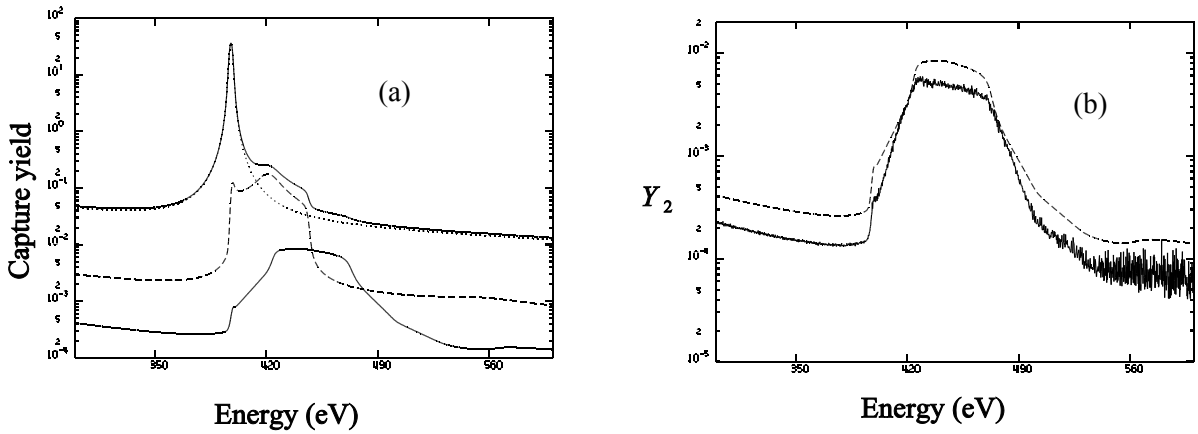

Figure 5. Capture yield for the 398-eV $J^{\pi} = 2^{!}$ resonance in ^{35}Cl. In part a, the dotted curve represents Y_0, the dashed curve Y_1, the lower solid curve Y_2, and the higher solid curve is the sum of the three. SAMMY (dashed curve) and SAMSMC (solid noisy curve) for Y_2 are shown in part b.

Next is a fairly typical example of an isolated strong resonance, this being the 398-eV $J^{\pi} = 2^{!}$ resonance in ^{35}Cl. The sample contains natural LiCl, two isotopes of Li and two of Cl. Part a of Fig. 5 shows the three components of the capture yield. No picture is shown of the Monte Carlo vs analytic curves for Y_1, since the two curves overlap entirely. Part b of the figure shows the comparison of analytic (dashed curve) vs Monte Carlo (solid, noisy curve) for the double-plus scattering. Although the shape of the Monte Carlo curve is reproduced fairly accurately by the SAMMY calculation, the absolute magnitudes of the two curves are different; further work is needed to determine the source for these differences. Nevertheless, it is important to maintain perspective: in this example, the value of Y_2 is smaller by at least one order of magnitude from the value of Y_0 and Y_1, so the discrepancy is not crucial here.

It is not always true that the relative magnitude of Y_2 is small compared to Y_0 and Y_1. In one interesting example, the sample contains a mixture of natural Sm plus heavy water. Except for one large low-energy resonance of ^{152}Sm, most of the multiple-scattering corrections are due to the presence of deuterium and oxygen. The double-plus scattering correction Y_2 is nearly the same magnitude as the single-scattering correction Y_1; at some energies it is larger. This is illustrated in Fig. 6; part a shows the capture yield with and without inclusion of the heavy water in the calculation. Part b shows both the single-scattering correction (dashed curve) and the double-plus correction. Only the analytic curve is shown for the single-scattering, as it agrees well with the Monte Carlo curve. For the double-plus correction term, the analytic and the Monte Carlo calculations are in relatively good agreement though there are again small differences in magnitude.

Space does not permit illustration of results of comparisons for other samples (Ba and natural Si have been studied), or in other energy regions. A full report will be prepared containing these results as well as others.

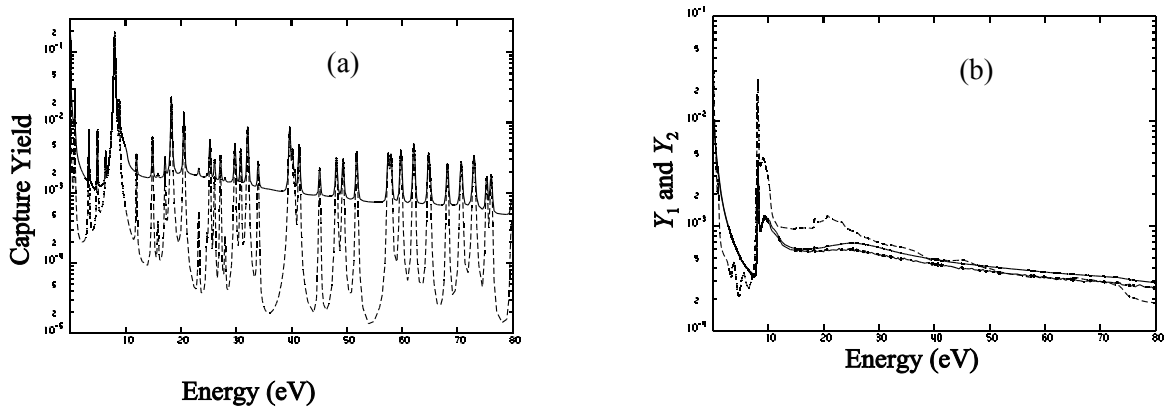

Figure 6. Capture yield for natural Sm plus heavy water. Part a shows the capture yield, both with the water included (solid curve) and without the water (dashed curve). Part b shows the multiple-scattering corrections to the capture yield. The dashed curve is the single-scattering correction (the curve is virtually the same for analytic and Monte Carlo). The solid smooth curve shows SAMMY's analytic approximation for the double-plus-scattering correction, and the noisy solid curve is the Monte Carlo calculation for that same quantity.

5. CONCLUSIONS

Comparisons between results for Y_i (i = 0, 1, 2) from SAMMY vs those from SAMSMC have been performed for a variety of samples. Results from these comparisons indicate that agreement between SAMMY and SAMSMC for Y_0 is excellent (as expected, since this is a trivial quantity to calculate). Agreement for Y_1 is also good. Agreement for Y_2 is, again as expected, not as good; nevertheless, the general shape (as a function of energy) of SAMMY's Y_2 calculation is similar to the shape of SAMSMC's Y_2 simulation. Further study is required in order to determine whether the differences are due entirely to the inadequacy of the approximations inherit in SAMMY's double-plus algorithm, or whether there remains a problem in the implementation of that algorithm.

If indeed the differences result from inadequacy of the approximations, one possibility exists for ad-hoc improvement in the SAMMY calculation of Y_2: a multiplicative factor for Y_2 could be determined by the analyst using SAMSMC/SAMMY comparisons, and provided as input into the SAMMY analysis. This possibility needs further exploration. The effect of uncertainties in the calculation should also be addressed, so that uncertainties in the final results accurately reflect calculational uncertainties as well as experimental uncertainties.

Finally, a systematic study is needed to determine limits of viability of the SAMMY approximations and implementations. First, the samples studied in this paper should be revisited, using different values for the sample thickness. (Perhaps it will be possible to develop a "goodness" criterion as a function of sample thickness, for a given nuclide or combination of nuclides.) Second, other nuclides should be studied, including known pathological examples such as ^{53}Cr in the energy range 2 to 10 keV [7].

ACKNOWLEDGMENTS

The authors gratefully acknowledge the influence and advice from the many SAMMY users who have encouraged this study. One of us (KNV) wishes to thank the International Atomic Energy Agency Fellowship Program for the grant which made possible his participation in this study.

REFERENCES

1. N. M. Larson, "Updated Users' Guide for SAMMY: Multilevel R-Matrix Fits to Neutron Data Using Bayes' Equations," ORNL/TM-9179/R5, Oak Ridge National Laboratory, Oak Ridge, TN (2000).
2. N. M. Larson, "Introduction to the Theory and Analysis of Resolved (and Unresolved) Neutron Resonances via SAMMY," N. M. Larson, *Proceedings the IAEA Workshop on "Nuclear Reaction Data and Nuclear Reactors: Physics, Design and Safety"*, International Centre for Theoretical Physics, Trieste, Italy, 23 February - 27 March 1998, pub. World Scientific, pp. 1-45 (1999).
3. F. H. Fröhner, *Nucl. Sci. Eng.* **103**, 119-128 (1989).
4. M. C. Moxon, "REFIT2: A Least Squares Fitting Program for Resonance Analysis of Neutron Transmission and Capture Data," NEA-0914/02, July 1989.
5. G. deSaussure, private communication (~1980).
6. F. G. Perey, private communication (~1985).
7. F. H. Fröhner, "Evaluation and Analysis of Nuclear Resonance Data," JEFF Report 18 (2000).